EXPERIMENTAL INVESTIGATION OF HIGH-TEMPERATURE, SHORT RESIDENCE-TIME CALCINATION AND SULFATION OF LIMESTONE AND DOLOSTONE SORBENTS

Naiyi Hu, Ye Liu, Sharon Falcone Miller and Alan W. Scaroni
The Pennsylvania State University
402 Academic Activities Building
University Park, PA 16802

Key words: sorbent furnace injection, calcination, sulfation.

INTRODUCTION

Sulfur dioxide emissions from coal-fired utility boilers and furnaces continue to be of significant regulatory concern. One approach to reducing these emissions that has received considerable attention[1-4] is the injection of dry, pulverized sorbent (limestone or dolostone) into the combustion chamber. This technology has been applied to conventional coal-fired utility boilers[1,2] and is considered to be a good candidate for use in coal-fired heat engine applications.[3,4] During the process, the injected limestone or dolostone particles are rapidly heated by the hot combustion gases and calcined by the reactions $CaCO_3 \rightarrow CaO + CO_2$ and $CaMg(CO_3)_2 \rightarrow CaO + MgO + 2CO_2$, respectively. The CaO produced then reacts with SO_2 and excess O_2 in the combustion gases to form $CaSO_4$.

Experimental data on the rates of calcination, sintering and sulfation have been reported by Borgwardt and others.[5-8] The physical structure of the calcined sorbents has also been investigated,[5,9,10] and a number of models have been developed describing the calcination and sulfation processes.[10,11,12] The primary application of dry sorbent injection is to conventional coal-fired utility boilers. The sorbent particle size used is either small (in the range of 1 to 30 μm) in pulverized coal applications or large (in the range of 0.25 to 1 mm) for fluidized-bed applications. Few investigations have been carried out using 30 to 100 μm particles, which is the size range of interest for coal-fired heat engine applications.[3,4]

This study investigated the calcination and sulfation behavior of three different sorbents (two limestones and one dolostone) in the size range from 37 to 105 μm. The time required for heating and calcination, the effect of the calcination process on sulfation behavior, and the effect of sorbent type on sulfation behavior were of primary interest.

EXPERIMENTAL

The calcination and sulfation experiments were conducted in the entrained-flow reactor illustrated in Figure 1. It consists of a preheater, a side-heated sorbent injector, and a vertical reactor. The preheater, injector and reactor were electrically heated to provide the desired gas preheating temperature and reactor temperature. The inside diameter of the ceramic reactor tube is 50.8 mm and it has an isothermal zone length of 600 mm. Dry air was used as the entrainment gas and was preheated to the same temperature as that in the reactor isothermal zone (±13 °C). The total gas flow rate was 60.7 l/min. As the preheated air passes through the injector section, the heat loss caused by contacting the injector wall is compensated for by the heat transferred from the heating wire wound around the outside of the injector. The sorbent was fed by a calibrated fluidized bed feeder. Room temperature air was used for sorbent injection and it comprised 5 % by mass of the total air flow to the reactor. A flow stabilizer was used to eliminate pulsations of the feed material caused by the fluidized feeder. SO_2 was doped into the gas flow by a mass flow controller to provide an SO_2 concentration of 2000 ppmv in the reactor. The sorbent feed rate was adjusted to achieve a Ca/S molar feed ratio of 2.0. Solid samples were collected through a nitrogen-purged, water-cooled sampling probe. During sampling, the nitrogen was used to increase the cooling rate of the sample. The nitrogen comprised 50 % of the total gas flow through the probe. Calculations indicated that 89 μm particles were cooled from 1,100 to 700 °C within 0.03 second after entering the sampling probe.

The stratigraphic formations, chemical compositions and the specific BET surface areas of the two limestone and one dolostone sorbents tested are shown in Table 1. The materials were crushed and wet sieved to size fractions of 74-105 μm (140x200 US mesh), 53-74 μm (200x270 US mesh) and 37-53 μm (270x400 US mesh). The sieved materials were dried in an oven at 105 °C for 48 hours.

The solid samples extracted from the reactor were analyzed for loss-on-ignition (using a Leco MAC-400 proximate analyzer), BET surface area (using a Quantachrome Autosorb-1 analyzer system with nitrogen), and sulfur content (using a Leco SC-132 sulfur analyzer with V_2O_5 catalyst). Some hydration occurred during sample collection and transfer. The extent of hydration was determined (using the Leco MAC-400 proximate analyzer) and the calcination and sulfation data corrected accordingly.

RESULTS AND DISCUSSION

CALCINATION BEHAVIOR

The extents of calcination of the Linden Hall limestone at gas temperatures of 1,000 and 1,100 °C are shown in Figures 2 a and b, respectively. The initial calcination rate is slow, followed by a rapid increase, and then a decline as the calcination process approaches completion.

An initial slow rate of calcination was observed for all three sorbents studied and this was attributed to the use of ambient air as the injecting medium, and the time needed for the sorbent particles to reach their decomposition temperatures.

Effects of Ambient Air Sorbent Injection and Time Required for Particle Heating: Sorbent injection systems typically use ambient air as the injecting medium. To simulate this condition, the sorbents were entrained in air at room temperature. As previously indicated, the sorbent-entraining air comprised 5 %, by mass, of the total air flow to the reactor tube. This ambient air, when mixed with preheated air in the top of the reactor, reduced the reactor inlet temperature. Figure 3 shows the measured gas temperature profiles along the reactor. It was found that the gas temperature, at a location corresponding to 0.1 second after injection, was 40 °C lower than the gas temperature at the same location when no ambient air injection occurred. The lower inlet gas temperature caused by the ambient air injection resulted in a delay in the initial calcination of the sorbents.

Another reason for the significant delay in calcination was the heating time required for the relatively coarse sorbent particles to reach their decomposition temperature. Figure 4 shows the calculated temperature profiles of 10 and 63 μm particles as a consequence of convective heat transfer. It takes much longer for the relatively coarser sorbent particles (in the range of 37 to 105 μm) to heat up than for a 10 μm particle. The characteristic heating time for a 105 μm sorbent particle is 92 ms and that for a 10 μm sorbent particle is only 0.8 ms. This latter time is negligible for conventional utility boilers firing pulverized-coal where the effective sorbent reaction time is about 2 seconds. However, the characteristic heating time for 63 μm sorbent particles is 33 ms, which is significant in heat engine applications.

Effect of Sorbent Particle Size on the Calcination Process: Over the sorbent size range from 45 to 89 μm, the effect of particle size on the calcination process at 1,000 °C is shown in Figures 2 and 5. For the three sorbents studied, the extent of calcination was not significantly dependent on the sorbent particle size.

From the classical shrinking-core model, the extent of calcination can be expressed as:

$$x = 1 - (1 - k \cdot t / dp)^3 \qquad (1)$$

where dp is the particle diameter, k is the calcination rate constant and t is the calcination time. In Equation (1), the extent of calcination has a strong dependency on particle size. Borgwardt[5] demonstrated that, when the resistances of intraparticle and interparticle mass transfer were eliminated, the calcination rate of small limestone particles could be described by a model that assumed a direct relationship with the specific BET surface area of $CaCO_3$. This calcination model has the form:

$$d(CaCO_3) / dt = k \cdot S_g \cdot (CaCO_3) \qquad (2)$$

where $(CaCO_3)$ is the weight of the undecomposed carbonate and S_g is the specific BET surface area of $CaCO_3$. By integration, the extent of calcination is related to the specific BET surface area by:

$$x = 1 - \exp (- k \cdot t / S_g) \qquad (3)$$

Milne et al.[10] employed a modified shrinking-core model to interpret the experimental data of Borgwardt[5]. A good fit was obtained when the particle diameter dependency was reduced to the 0.6 power, and the empirically modified equation was:

$$x = 1 - (1 - k \cdot t / dp^{0.6})^3 \qquad (4)$$

Comparison of the calcination models with the experimental data for the Linden Hall limestone at 1,000 °C is shown in Figure 6. This data indicate that the calcination model based on the specific BET surface area of $CaCO_3$ is a better predictor of the experimental data than the modified shrinking core model. A comparison of the calcination models with the data for the Bossardsville and Nittany sorbents results in the same conclusion.

To be able to apply the modified shrinking-core model to the experimental data of this study requires that the particle size dependency be reduced to a power of between 0.2 to 0.3, depending on the particular sorbent. The very weak particle size dependency implies that these sorbents had very rough surfaces and the different size dependencies of the different sorbents may be related to the physical structures of the sorbents as well as to the chemical reactions that occur on the surface. This issue will be clarified in future studies.

SULFATION BEHAVIOR

The sulfation data for the three sorbents at a gas temperature of 1,000 °C are shown in Figure 7. The extent of sulfation is expressed as the molar ratio of sulfur to calcium in the solid sample. The data reveal that the sulfation process for the limestone and dolostone particles in this size range was different than that associated with small particles (~5 μm) and precalcined sorbents.[13] There were no initial rapid sulfur capture periods as was the case for most small particles and precalcines.[13] The sulfation rates increased steadily and monotonically. In addition, the low calcium dolostone exhibited a greater sulfur capture capability than the high calcium limestone for the same experimental conditions. The 1,100 °C sulfation data for the three sorbents showed the same trends.

Effect of Calcination Rate on Sulfation Rate: Figure 8 shows the calcination and sulfation curves for 45 μm Bossardsville limestone particles at a gas temperature of 1,000 °C. The experimental

data of Cole et al.[13] using precalcined limestone at similar sulfation conditions are also shown in Figure 8 (indicated by the square data points). Comparing the sulfation curves of the 45 μm limestone particles used in this study and that of Cole's study, the initial rapid sulfur capture period, typical of precalcines and small particles, was not apparent. Based on the calcination curves generated in this study, it is concluded that the delay in calcination is responsible for the initial lower extent of sulfur capture. For the 63 μm Bossardsville limestone particles, the extent of calcination was only 8 % for a 0.2 seconds particle residence time. Though the sulfation rate of the CaO produced was very high, there was not sufficient CaO available at that time for extensive sulfation to occur. As a consequence, the sulfur capture (based on the molar ratio of sulfur to calcium) was low. Despite the initial sulfation delay, the slope of the sulfation curve at longer residence times did not level off. The ongoing calcination process produced fresh CaO surface to be sulfated. The production of a $CaSO_4$ layer from the CaO initially produced resulted in a slower rate of sulfation due to product layer diffusion limitations. However, the sulfation rate of newly created CaO was rapid, thereby compensating for the slower rate of sulfation of the CaO beneath the $CaSO_4$ layer. For particle residence times up to one second, which corresponded to an 80 to 90 % extent of calcination, no significant decrease of the apparent sulfation rate was observed.

Effect of Sorbent Type on Sulfation: As shown in Figure 7, the different sorbents exhibited different sulfation performances at the same experimental conditions. For the sulfation tests with 45 μm particles at 1,000 °C and 1.1 second residence time, the calcium utilization of the Linden Hall limestone was 9 %, that of the Bossardsville limestone was 12 %, while that of the Nittany dolostone was 28 %. On the basis of sorbent utilization (rather than calcium utilization), the performance of the lower purity Bossardsville limestone was not significantly different than that of the high purity Linden Hall limestone. The Nittany dolostone, which contained only 50 % calcium carbonate, displayed better performance than the high purity Linden Hall limestone. At a Ca/S molar feed ratio of 2.0, the 45 μm Nittany dolostone particles reduced the SO_2 in combustion gas by 56 % in 1.1 seconds at 1,000 °C.

CONCLUSIONS

1. Simulating the dry sorbent furnace injection process by using ambient temperature air as the injection medium increased the heating time of 37 to 105 μm diameter particles and delayed the calcination process.
2. The extent of calcination was insensitive to particle size in the range studied. The calcination model based on the specific BET surface area of the raw sorbent produced the best fit of the experimental data.
3. The calcination delay significantly affected the apparent sulfation rate for up to 0.2 seconds after sorbent injection. Between 0.2 and 1.0 seconds, the apparent sulfation rate was almost constant.
4. High purity limestones may not be the best choice for use in dry sorbent furnace injection processes. Low calcium dolostone may display better sulfation performance.

ACKNOWLEDGMENTS

Financial support for this work was provided by Manufacturing and Technology Conversion International, Inc. under DOE Contract #DE.AC21-89MC26288. The cooperation of the staff of The Combustion Laboratory is also acknowledged.

REFERENCES

1. Proceedings: *1990 SO_2 Control Symposium,* Session 3A, EPRI GS-6963, Electric Power Research Institute, Sept. 1990
2. Proceedings: *First Combined Flue Gas Desulfurization and Dry SO_2 Control Symposium,* Session 4A, EPRI GS-6307, Electric Power Research Institute, April 1989
3. Abichandani, J. S., *Gas Stream Cleanup Papers from DOE/METC Sponsored Contractors Review Meetings,* DOE/METC-89/6099, Morgantown, WV, 1988, p.167
4. Lawson, W. F., Maloney, D. J., Shaw, D. W. Richards, G. A., Anderson, R. J., Cook, J. M., Siriwardane, R. V., Poston, J. A. and Colaluca, M. A., *Proceedings of Seventh Annual Coal-fueled Heat Engines and Gas Stream Cleanup Systems Contractors Review Meeting,* DOE/METC-90/6110, Morgantown, WV, 1990, p.283
5. Borgwardt, R. H., *AIChE J.*, 1985, **31**, 103
6. Borgwardt, R. H. and Bruce, K. R, *AIChE J.*, 1986, **32**, 239
7. Borgwardt, R. H., Roache, N. F. and Bruce, K. R., *Ind. Eng. Chem. Fundam.*, 1986, **25**, 165
8. Powell, E. K. and Searcy, A. W., *Metallurgical Trans.*, 1980, **11B**, 427
9. Newton, G. H., Chen, S. L. and Kramlich, J. C., *AIChE J.*, 1989, **35**, 988
10. Milne, C. R., Silcox, G. D. and Pershing, D. W., *Ind. Eng. Chem. Res.*, 1990, **29**, 139
11. Milne, C. R., Silcox, G. D. and Pershing, D. W., *Ind. Eng. Chem. Res.*, 1990, **29**, 2201
12. Dam-Johansen, K., Hansen, P. F. B. and Østergaard, K.,*Chem. Eng. Sci.* 1991, **46**, 847
13. Cole, J. A., Kramlich, J. C., Seeker, W. R., Silcox, G. D., Newton, D. W., Harrison, D. J. and Pershing, D. W., Proceedings: *1986 Joint Symposium on Dry SO_2 and Simultaneous SO_2/NO_x Control Technologies,* Vol. 1, 16-1, EPRI CS-4966, Electric Power Research Institute, Dec. 1986

Table 1. Stratigraphic formations, chemical compositions and BET surface areas of the sorbents

Formation	$CaCO_3$	$MgCO_3$	SiO_2	Al_2O_3	Fe_2O_3	BET surface area (m^2/g)		
						45μm	63μm	89μm
Linden Hall	99.42	0.86	0.69	0.31	0.07	0.422	0.396	0.351
Bossardsville	86.93	1.91	8.07	1.46	0.95	0.648	0.613	0.579
Nittany	49.62	39.30	8.01	1.41	0.53	0.534	0.477	0.376

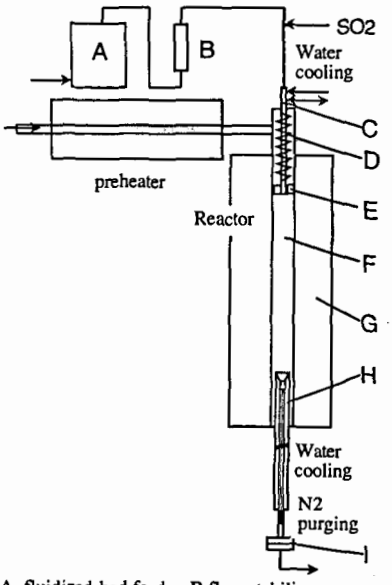

A fluidized-bed feeder, B flow stabilizer
C sorbent and SO2 injector
D injector outside heating
E flow straightener, F reactor tube
G electric furnace, H solid sampling probe
I sample filter

Fig. 1 Schematic diagram of entrained-flow reactor

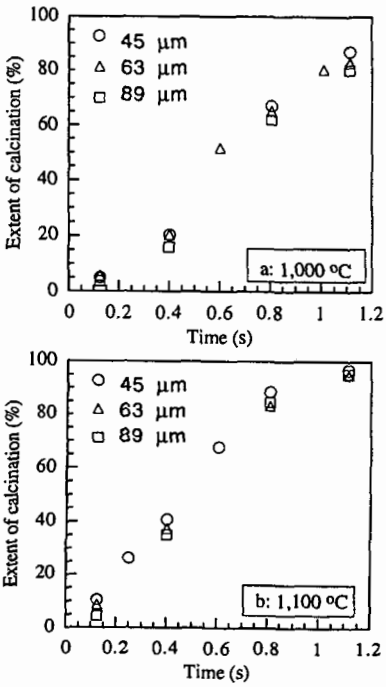

Fig. 2 Time dependency of the extent of calcination of the Linden Hall limestone at a) 1,000°C and b) 1,100°C for various particle sizes

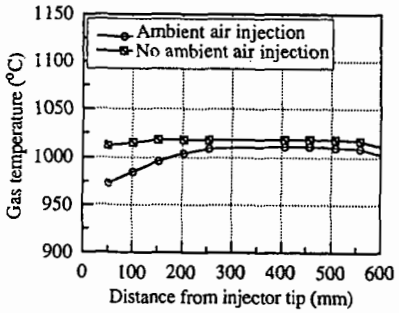

Fig. 3 Effect of injecting sorbent with ambient air on the gas temperature profile along the reactor

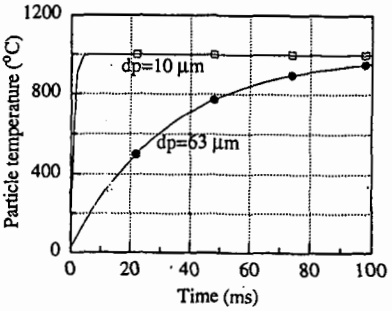

Fig. 4 Calculated sorbent particle temperature profiles during convective heating for 10 and 63 μm particles

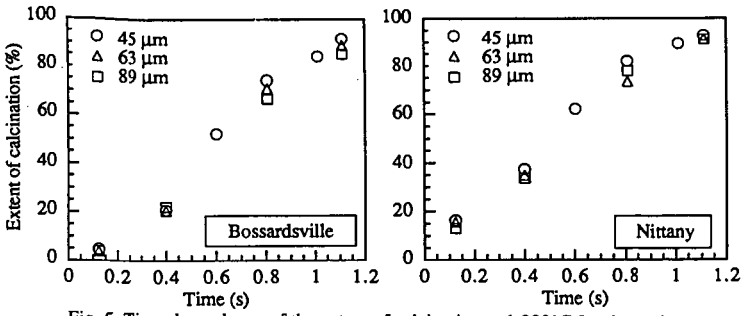

Fig. 5 Time dependency of the extent of calcination at 1,000°C for the various particle sizes of the Bossardsville and Nittany sorbents

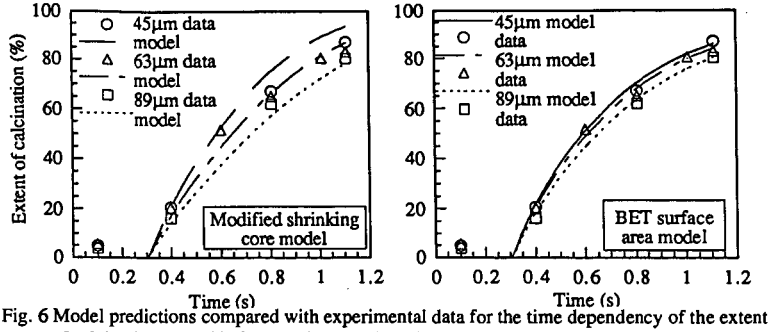

Fig. 6 Model predictions compared with experimental data for the time dependency of the extent of calcination at 1,000°C for various particle sizes of the Linden Hall limestone

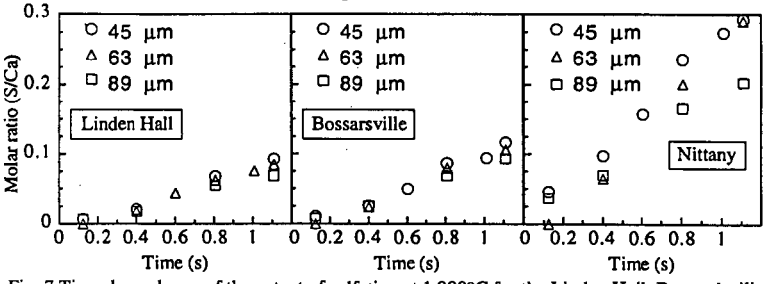

Fig. 7 Time dependency of the extent of sulfation at 1,000°C for the Linden Hall, Bossardsville and Nittany sorbents

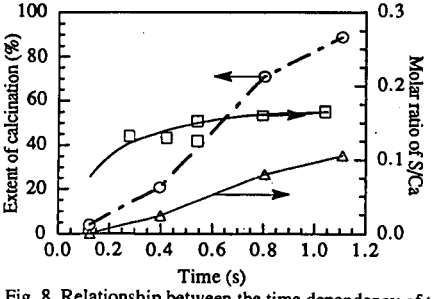

Fig. 8 Relationship between the time dependency of the extents of calcination and sulfation at 1,000°C of 63 μm Bossardsville limestone particles